LCC-0156
SLAC-PUB-10883
Jan. 2005

Linear Collider Collaboration Tech Notes

Localization of RF Breakdown in Copper RF Structure by the Use of Acoustic Sensors

F. Le Pimpec, J. Frisch, K. Jobe,
D. McCormick, J. Nelson, M. Ross, T. Smith

Stanford Linear Accelerator Center
Menlo Park, CA 94025

Abstract: X-band accelerator structures meeting the Next Linear Collider (NLC) design requirements have been found to suffer damage due to Radio Frequency(RF) breakdown when processed to high gradients [1]. Improved understanding of these breakdown events is desirable for the development of structure designs, fabrication procedures, and processing techniques that minimize structure damage. Acoustic sensors attached to an accelerator structure can detect both normal and breakdown RF pulses [2]. Using an arrayof acoustic sensors, we have been able to pinpoint both the cell and azimuth location of individual breakdown events. This allows studies of breakdown in time and in space, so that underlying causes can be determined. This technique provided a significant understanding of breakdown in the structure input coupler.
Key words: Acoustic Sensor, Acoustic Wave, RF Breakdown, Copper Structure, RF Structure, X-band, Phonon

Localization of RF Breakdown in Copper RF Structure by the Use of Acoustic Sensors

F. Le Pimpec [1]
J. Frisch, K. Jobe, D. McCormick, J. Nelson, M. Ross, T. Smith

SLAC, 2575 Sand Hill Road Menlo Park CA 94025 , USA

Abstract

X-band accelerator structures meeting the Next Linear Collider (NLC) design requirements have been found to suffer damage due to Radio Frequency (RF) breakdown when processed to high gradients [1]. Improved understanding of these breakdown events is desirable for the development of structure designs, fabrication procedures, and processing techniques that minimize structure damage. Acoustic sensors attached to an accelerator structure can detect both normal and breakdown RF pulses [2]. Using an array of acoustic sensors, we have been able to pinpoint both the cell and azimuth location of individual breakdown events. This allows studies of breakdown in time and in space, so that underlying causes can be determined. This technique provided a significant understanding of breakdown in the structure input coupler.

Key words: Acoustic Sensor, Acoustic Wave, RF Breakdown, Copper Structure, RF Structure, X-band, Phonon

1 Introduction

As part of the R&D effort for the Next Linear Collider (NLC), the reach of high gradients (70MV/m) with a breakdown rate of 1 per 10 hours must be demonstrated [3] [4]. In the Next Linear Collider Test Accelerator (NLCTA), at SLAC (Stanford Linear Accelerator Center), RF travelling waves, but also standing wave, copper structures designed to meet the needs of the NLC [5] were tested.

[1] E-mail: lepimpec@slac.stanford.edu

To reach an NLC accelerating field of 70MV/m with a 400ns pulse length, Megawatt of RF power is poured into the structures. Depending on the design and type of the structure, this power can vary from 73MW for a 60cm long travelling wave structure with a 3% group velocity (H60Vg3) to 150MW for some of the first structure of 180cm long. A part of this RF power is lost in the copper and transformed into heat. The lost power is up to 2/3 of the input power for a structure kept at 45°C. The thermal expansion of the copper, as the structures fill with RF power, causes sound and thus on every machine pulse. Using extremely sensitive piezoelectric microphones, or acoustic sensors, it is possible to "listen" to the accelerator structure as it is running, cf Fig.1.

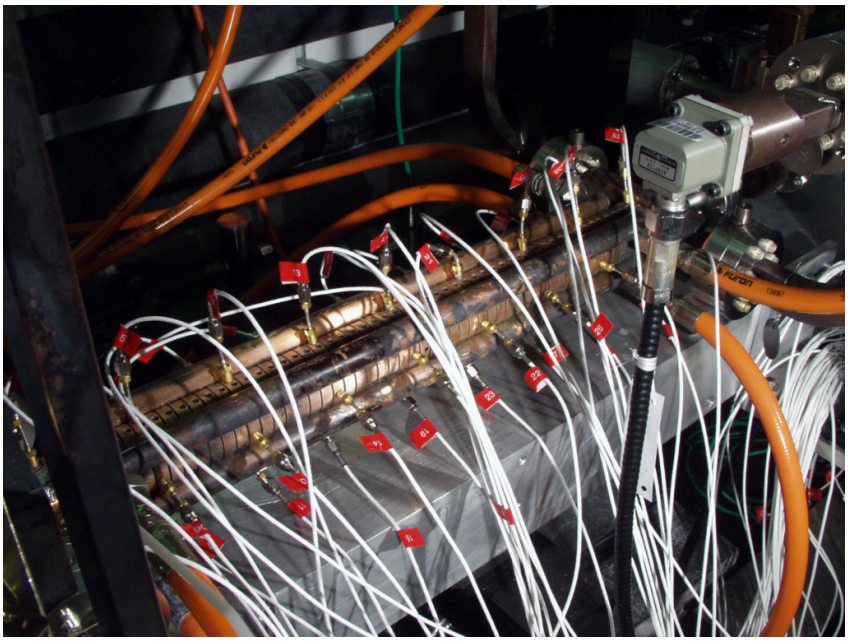

Figure 1. T53VG3RA (53cm long travelling wave structure of 3% group velocity) structure plastered with Acoustic sensor

The obtention of high gradient is obtained by exposing the structure to High Power Pulsed RF (HPP). This technique is called RF processing. During processing the structures occasionally respond by arcing, or breakdown. A breakdown is characterized by a shut off of the transmitted power and up to 80% of the incident power is absorbed in the arc [6]. This extra energy is deposited in the copper, and a part of it is converted in extra phonons (heat and acoustic) that can be picked up by our acoustic sensors. With this technique, crude localization of a breakdown is straight forward, and complementary to the standard RF analysis with directional RF couplers. As the RF analysis of a breakdown signal can provide its localization on line, it seems that using acoustic sensor to locate breakdown is superfluous. We will, however, show how acoustic sensor are not only complementary of RF analysis, but how they did impact on the reach of high gradient.

2 Breakdowns, Copper and Acoustic Limitation

For achieving the designed parameter of the accelerating voltage needed for NLC, the RF accelerating structure are subject, before HPP, to a series of chemical and heat processing, which can be called pre-processing. This pre-processing is suppose to "clean" the surface from contaminants which can trigger RF breakdown. The use of acoustic sensor in the domain of accelerator is rather new and it seems reasonable to summarize briefly the implication of the pre-processing on the acoustic propagation.

After the chemical etching of the cells structures are either bonded in an hydrogen atmosphere (SLAC treatment) or brazed under argon atmosphere (FNAL treatment). Any gas dissolved in the copper is outgassed by a vacuum firing. The temperature involves in the thermal treatment varies from 600°C to 1000°C. At these temperatures, grains are growing and recrystallization occurs. The speed of sound in copper is dependant of the form and of the treatment received by the copper [7]. Hence, the grain size of the material being a limiting factor, due to the diffraction of the waves, for the choice of an acoustic sensor. The copper RF structure have a typical grain size of the millimeter. For a pressure waves of 4760 m/s [7] the diffraction limit is achieved at 4.7 MHz. Local plasticity due to the intake of hydrogen, can also affects the propagation of the acoustic waves inside the copper [8]. It is not clear if the vacuum firing will relax the crystalline structure of the copper.

The choice of an adequate sensors for localization is then dependant, not only of the pickup properties of the sensor but also of the frequencies of the acoustic waves to be analyzed. Hence, resolution which can be achieved by an array of these sensors depends of the diffraction limits, the attenuation... of the different type of waves, pressure waves, shear waves and surface waves (Rayleigh waves) [9] [10] as well as any anisotropy of the medium [11]. Finally the complex geometry of the cells forming the structure is also an extra challenge to the resolution, Fig.2.

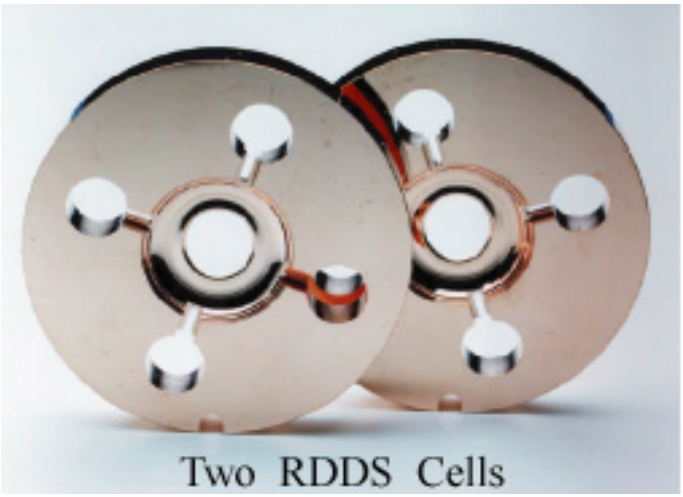

Figure 2. Rounded Damped and Detuned NLC type accelerator cell structure

3 Acoustic Sensors & Data Acquisition System

3.1 Acoustic Sensors

Since the first report on this technique [12] several commercial, the same kind of sensor used to monitor microscopic cracks in bridges or airplane frames, as well as SLAC-made sensors, Fig.3, have been tested and used [13].

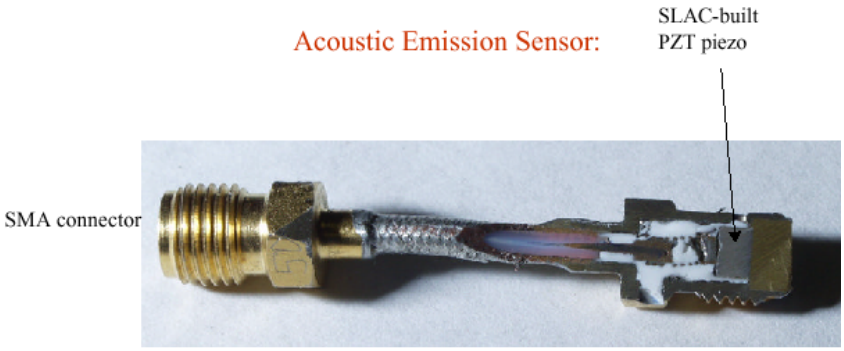

Figure 3. SLAC type Acoustic Sensor 200Khz - 1.5 MHz

Most of the results presented in this paper were obtained using the sensor shown in Fig.3. The sensor is made of a piezoelectric ceramic solder on a copper piece. A conductor is then soldered on the back of the ceramic and connected to an SMA connector. The surrounding of the ceramic is embedded in a Room Temperature Vulcanizing (RTV) silicon which act as a damping material. A power response in dB versus frequency of the sensor is given in Fig.5 when driven by a commercial microdot 100 sensor. The sensor are glued on the structure by the use of fast drying Loctite. The use of a hardener, sprayed on

the structure when the sensor are pressed onto it help getting a good contact. With this technique, we also obtain a better reproducibility of the contact between the sensor and the copper structure. Loose or shaky contact often leads to a drastic reduction of the recorded signal. Due to our requirements, we are now using commercial sensors ITC-9070 from *International Transducer Corporation*.

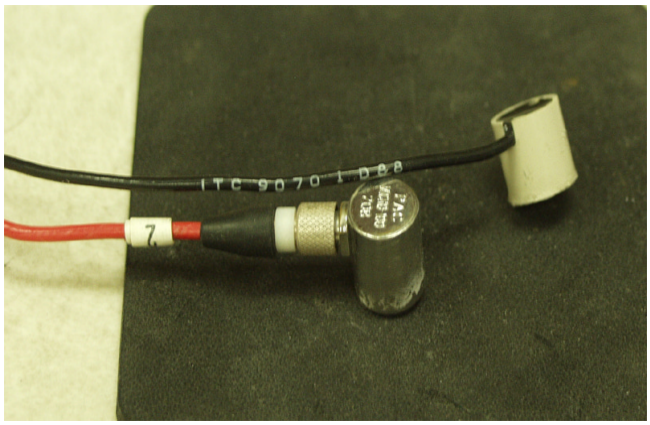

Figure 4. Microdot 100 and ITC 9070 (white sensor with black cable)

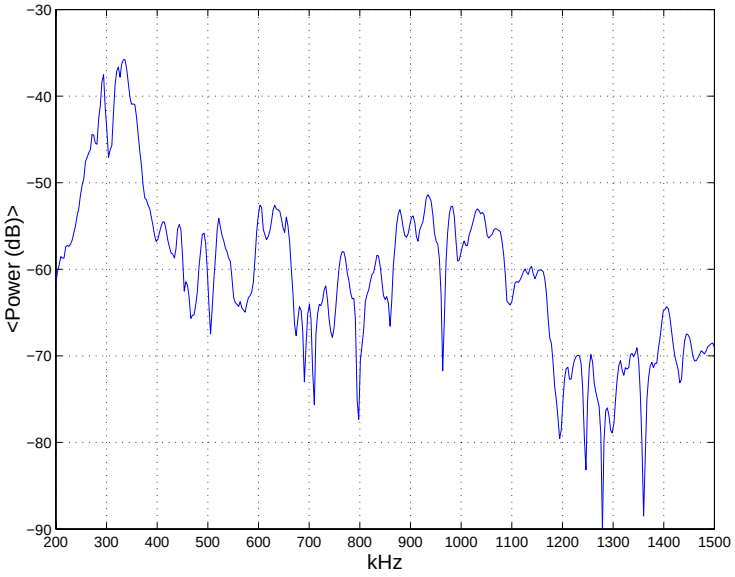

Figure 5. Homemade SLAC sensor frequency response, when driven by a Microdot 100 Sensor. The signal is analyzed via a network analyzer. Sensors are held together with a pinch clamp and vacuum grease in between.

3.2 Electronics and DAQ System

An array of up to 64 sensors (limited by DAQ channels) is attached to the accelerator structure to locate breakdowns. Radiation in the accelerator tunnel prevents the use of local electronics and the sensors are transformer coupled

to drive differential pair cables. A differential receiver and amplifier are used in the control area, followed by a digitizer.

3.3 Analog Electronics

The acoustic sensors act approximately as current sources in parallel with about 1000pf of capacitance. For 300KHz signals this corresponds to 500 Ohms impedance. The sensor is connected to a 400:100 Ohm transformer driving 100 Ohm twisted pair (Cat-5 Telecom) cable, with impedance matching to 50 Ohms at the receiver. The Cat-5 is useful because it does not pick up noise and has a low cost. A variable gain amplifier is used to match the signal level into the digitizer input. [13]

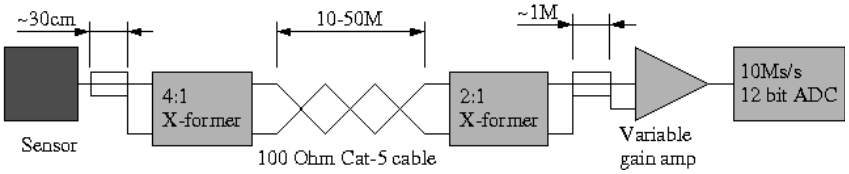

Figure 6. Electronics block diagram

3.4 Digital Electronics and Software

The Digitizers used are Joerger VTR812-10, 8 channel, 12 bit, 10Ms/s VME modules the input range is ± 2 volts, 50 ohm input. Eight modules were used for a total of 64 channels. The modules are operated in circular buffer mode to record the last 3 events, with 1024 points per event, as represented in Fig.7. The n pulse being the RF pulse when the structure breakdown, the (n-1) and (n-2) pulses should be normal pulses, or background noise of the RF power. The control system is based on EPICS® and operates both the RF level control for processing and the acoustic data acquisition. When the processing system detects a RF breakdown, the next RF pulse is disabled and the data from all of the digitizers for the last three pulses is recorded. Data is processed offline using Matlab®. Typically the RMS of the first 200 points (20 μs or 10 mm at copper P-wave velocity 4760 m/s) is used to determine the breakdown location.

4 Sensor Calibration

Absolute calibration of acoustic sensors is not trivial in the frequency range of interest, some of the problem arises due to the imperfect nature of the

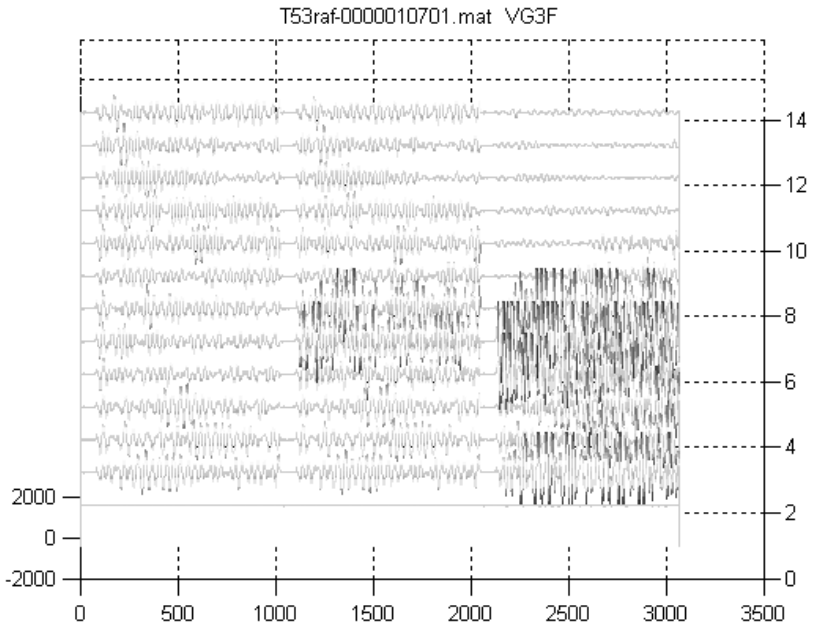

Figure 7. Sequence of 3 pulses in T53VG3F structure

transfer block used in between the sensors. Also, the repeatability between measurements after dismounting the system and remounting is poorer than without remounting [14]. A way we found to calibrate our sensor is to use the RF power dissipated in our copper structure. The RF losses inside the structure will induce a mass movement of the copper due to thermal expansion. The rise of temperature, of the overall accelerating structure, cooled with water, is slow and only of a few °C. It is then reasonable to keep the thermal properties of the copper constant during the RF pulse. We expect a response of the sensors linear with the power loss in the structure [12]. Results with RF pulses at 100 ns, 170 ns, 240 ns and 400 ns have been recorded for three structures and one set of results is displayed in Fig.8. The measurement, Fig.9, were carried out by taking artificial trigger, in order to avoid data corrupted by RF breakdown.

The RMS response in mV of the sensors versus the RF power flowing inside the structure, Fig.8 as example, confirms the results obtained in [12]. Results obtained for the sensors at other RF pulse length are similar. Data can be fitted with a linear equation showing the dependencies of the effect of the thermal heating by the RF vs the acoustic response of the sensor. We can see in Fig.8 the very good agreement between the data and the linear fit. Fig.10 displays the standard deviation [15] of the difference between the data set and its fit, and thus for the 64 sensors. The results shows that the difference between the data and the fit is around 2mV (blue cross and red circle). However, some sensor have a much larger deviation (red circles). Fig.11 displays the difference at a given power between the data and their fit for the 64 sensors (the error bar is the response in mV of the sensor). The data Set #2 at a RF power of

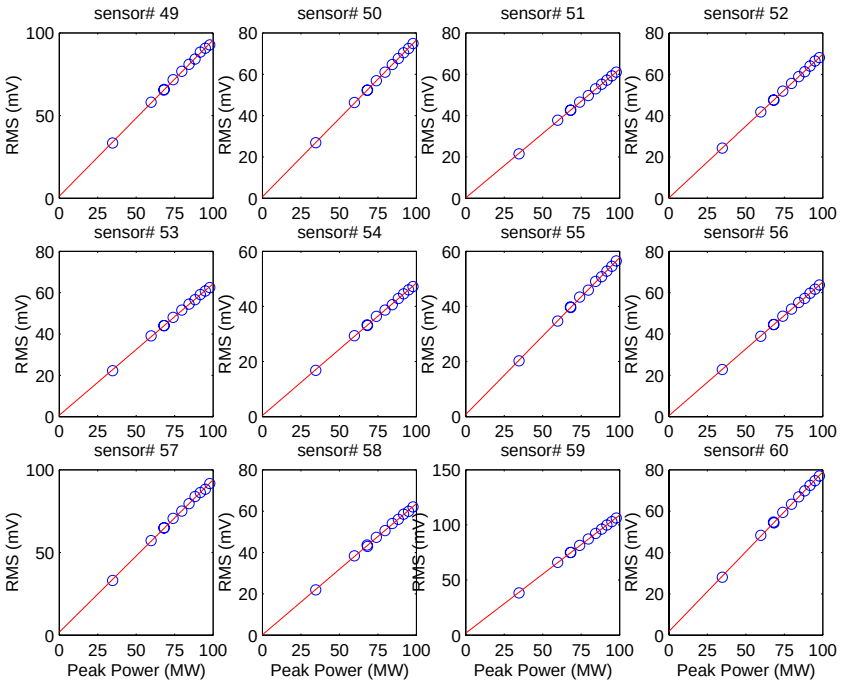

Figure 8. ITC-9070 sensor calibration with a 400ns RF pulse length with various RF power in H60VG3R structure. RMS of the first 20μs of the signal. The red line is a linear fit

58MW has a variation of the response which is much larger that at any other RF power : 20mV compare to 2mV. Thus the real accuracy of the fit to the data in Fig.8 is given by the blue cross set in Fig.10, withdrawing from the calculation of the standard deviation the set of data #2.

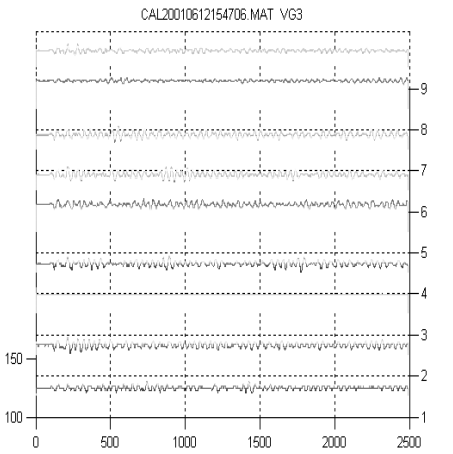

Figure 9. Acoustic sensors response to a 100ns RF pulse length and 150MW RF power in T53VG3R structure

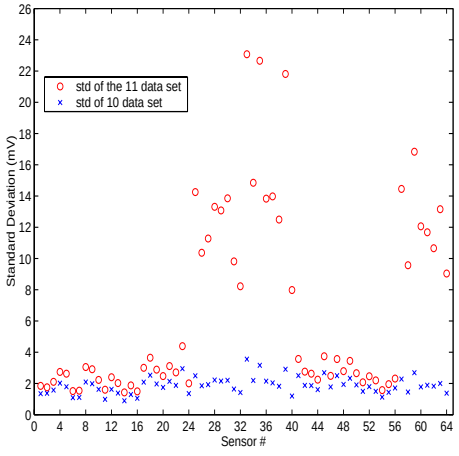

Figure 10. Standard deviation of the difference between the data set of a given sensor and its associated fit

In some cases, the expected trend was not obtained for some sensors. In those cases a bad contact between the sensor and the structure or a deficient sensor was responsible. As an example, Fig.9 displayed a typical response of acoustic

sensors when a normal pulsed RF feed the structure. A defective sensor, #3 in Fig.9, shows a flat line. This line is superimposed with the dotted grid axes labelled 4.

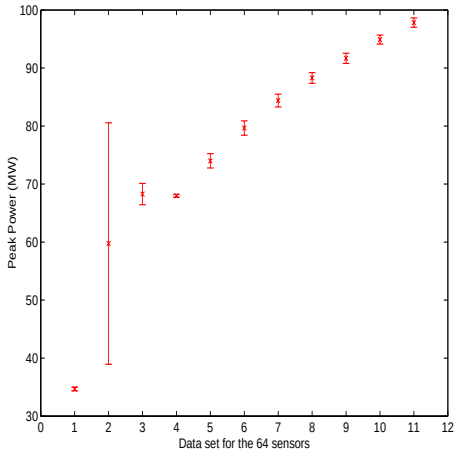

Figure 11. Standard deviation of the dif- ference between the response in mV of the 64 sensor and their associated fit at a given power

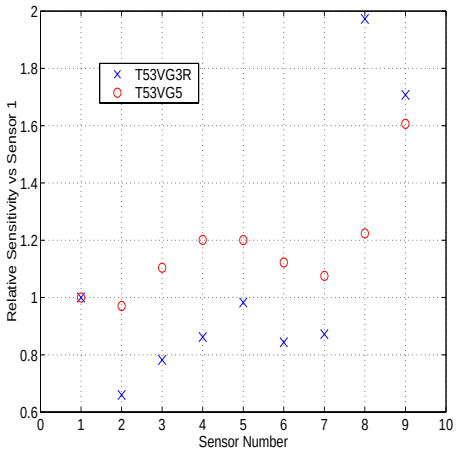

Figure 12. Sensitivity of the sensors relative to sensor 1 for T53VG3R (crosses) and T53VG5R (circles) structure

The purpose of doing a High Power Pulsed processing (HPP) [16], or RF processing, is to reach a given electric field value without arcing in the structure. Since data reduction is performed offline, sensor calibration can be performed after the end of the processing of the structure, or before switching from one RF pulse length to another. Maxwell equation and calculation of the loss of RF power in the copper structure without breakdown linked to this calibration curve might be a way to account for energy deposition in the structure when an arc occurs.

It has to be noted that simple calculation will show that the radiation pressure of the RF wave can be neglected in front of the sound wave created by the rise of temperature in the structure due to RF losses.

As an absolute calibration is not yet in reach, we might use a relative calibration, Fig.12. A set of data is recorded at a given pulse length and a ratio of the output of the voltage versus one of the sensor is calculated. The data are recorded in 3 slides of 1024 points corresponding to three consecutive RF pulses, Fig.7. We have chosen to calculate the sensitivity based on the first 200 points or 20μs of the signal.

As we can see in pulse (n-1), Fig.7, breakdown can occur without shutting off the klystron. Normally, when the accelerator software "detect" a breakdown, the power in the klystron is shut down for the next minute, and the acoustic data are recorded. It is then better to use the (n-2) pulse to calculate the relative sensitivity after each breakdown. However, in some very rare case, we

have seen breakdown in pulse (n-2), less than a %. Also, during operation sensors can fall off the structure, or broke, as the first sensor in Fig.7. Since data are not looked in a day to day basis but analyzed automatically, we might not be able to fix the problem in a reasonable time. Also as the processing evolves, the sensors are exposed to higher X-rays doses and we should consider the possibility that the initial relative calibration shift with time. Whatever are the mechanisms inducing a shift in the response of the sensor, we will refer to them in a general term of "ageing" of the sensors.
For most of our analysis some general relative sensitivity files were used. These files were updated time to time to take into account the ageing of the sensors. We did find out that results of coarse localization of breakdown using or not using those file were very similar. Precise localization, like localizing where on a cell the breakdown has dropped the most energy, required frequent update of these files.

5 Results & Discussion

5.1 Limitation of the SLAC-made sensors

In the frequency range of the SLAC-made sensor, Fig.3 and Fig.5, the wavelength of the phonon lies between 2.4 cm at 200 kHz and 3 mm at 1.5 MHz, assuming the speed of the longitudinal wave of 4760 m/s ($\lambda = \frac{c}{\nu}$). Fig.13 shows the frequency response of sensor #6 (Pulse #3) of Fig.7 on the T53VG3F structure, after a breakdown close or at its location. Almost no signal is recorded for frequencies above 1 MHz despite the frequency range of the SLAC sensors (200 kHz to 1.5 MHz). However, those sensors have a power attenuation of 10 dB to 15 dB at frequencies above 1.2 MHz cf Fig.5.

If the sensors are placed to close from each other the low end frequency of the acoustic spectrum will not be resolved. As the radial dimension of the thickness of the iris is comparable to the wavelength of the phonon, diffraction of the wave might occur. The cells have an outside diameter (OD) of ∼58 mm and a vacuum beam OD aperture of ∼10 mm. The length of a cell is 8.75 mm. The thickness of a cell is ∼17.5 mm but the thickness of the iris in the cell is ∼1.3 mm, Fig.2. To avoid diffraction, we can use acoustic sensor with a higher passband frequency. It has to be mentioned that not all the structure which have been tested have cells of this dimension. However, values are close.

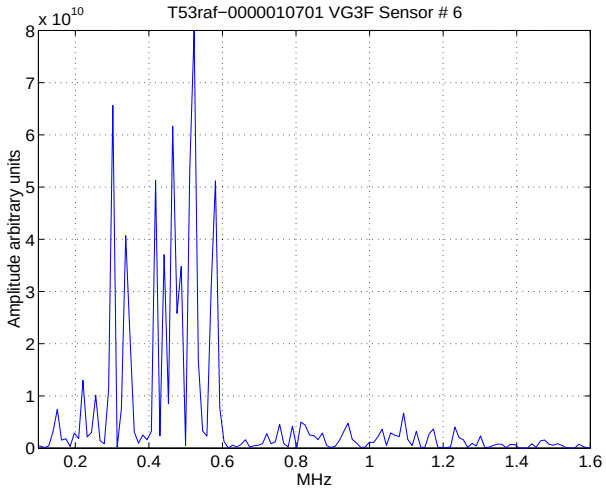

Figure 13. Fourier transform of the signal of sensor #6 after a recorded breakdown in Fig.7.

5.2 Acoustic Results

In Fig.7 a breakdown occurs in pulse#2 (n-1) in the middle of the T53VG3F structure, cell 25. The sensors were placed every 5 cells from the input coupler. This breakdown did not trigger the acquisition and is not accounted in the number of total breakdown occurring inside the structure. Also, on the pulse n we can detect 2 breakdowns. One is happening in the first 10 cells of the structure; the broken sensor 1 cannot allowed a more precise determination. The second breakdown is very probably located between cell 25 and 30. The second breakdown, in the same pulse, will not be accounted by the RF control software. By this example, we can see how the acoustic emission technique is complementary from the RF analysis of the reflected and transmitted RF power after a breakdown, to locate the cell where the breakdown happened [17].

Due to the quantity of data, it is necessary to automatically analyse the data. Simple analysis will calculate the RMS of the first 200 points of the n pulse. The biggest RMS value is then considered to be the location of the breakdown. From this sensor we can compare the other RMS and determine if the second highest RMS value is a valid second breakdown. This automatic method benchmarked with a manual scan of a given sample of data has given very good results. Fig.14 shows two histograms, one for the T53VG3RA (left) one for the T53VG3F (right) accelerating structures. Each of the plot displays the recorded number of breakdown or event during a given time of RF processing, versus the position in the structure where the event occurred. These results are in good agreement with the RF analysis, Fig.15. The green and red dots represents the breakdowns attributed to be happening in the input and output couplers. The blue dots are the events localized inside the body of the

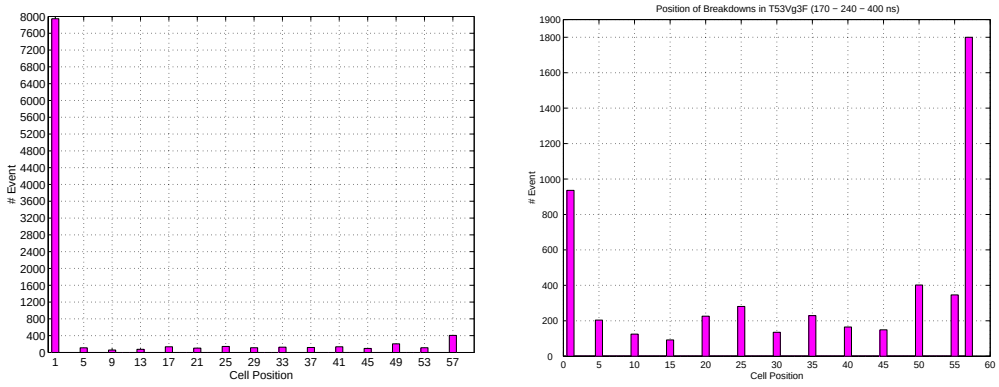

Figure 14. Number of single breakdown vs location of the 53 cm long RA (left) and F (right) travelling wave structure; for RF pulses of 170ns 240 ns and 400ns length structure.

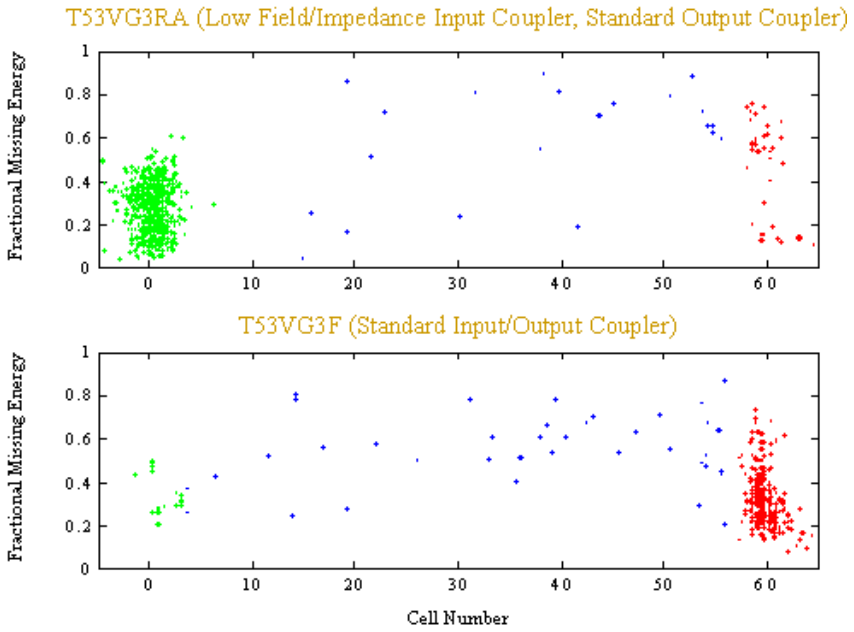

Figure 15. Localization of RF breakdown by the use of RF analysis. 120 Hours of operation, at 60 Hz repetition rate, 400 ns Pulse Width. Electric Field: 73 MV/m [17]

This crude analysis gives good coarse results on the localization of the breakdown. Finer results on the localization can be obtain in two ways.

- installing sensors on every cell.
- extrapolating, and interpolating, the results from the recorded data.

It is easier to install more sensors, however it is expensive in term of equipment. Refine analysis is then a preferable choice. From the raw data, a time analysis can be done. Looking at the bow shape of the signal, Fig.16, we can estimate where the location of the breakdown occurred, if we consider that the acoustic

wave is travelling in the copper structure in straight line and at the speed of sound.

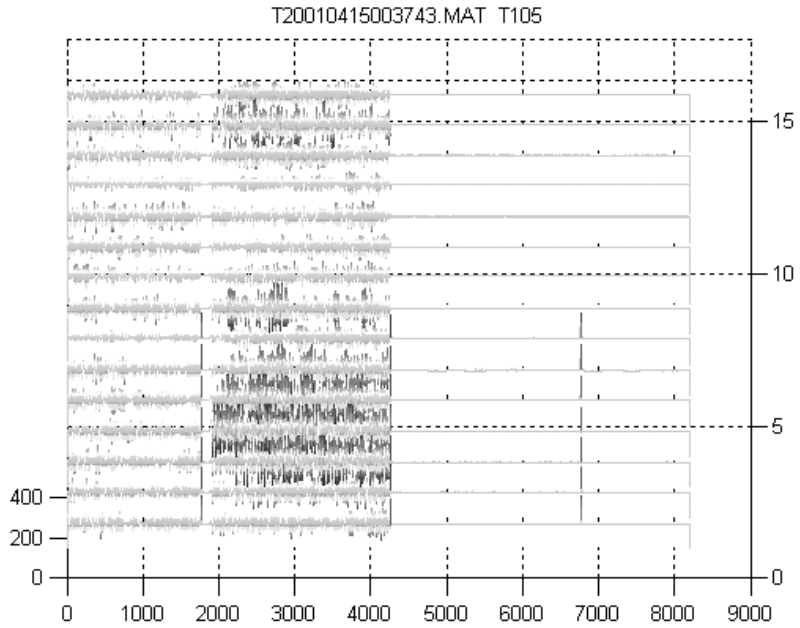

Figure 16. Multiple RF breakdown in T105VG5 travelling wave structure at 240ns pulse length. Sensors are located every 6 cells from cell #2

Manual data treatment of the timing information has given very promising results [12]. Automatic treatment of acoustic data in TTF (TESLA Test Facility) in DESY (Germany) [18] has allowed to locate, with few sensors, the origin of breakdown, Fig.17. Due to the complicated geometry of our structures, the automatic timing analysis with the NLCTA data is more challenging. To calculate the time for the breakdown signal to reach the sensor, first the integrated RMS of the first 20μs of the signal for the breakdown pulse (n pulse), and the RMS for a nominal non-breakdown event (2 pulses before, (n-2)) is calculated. Those two values are divided to get a normalized integrated RMS signal. This normalized value is subtracted to the mean of the first microsecond of the breakdown pulse signal for every sensor, giving an integrated RMS close to zero. During this first microsecond of the recorded signal, the RF is not yet switch on. The timing is obtained by having the ratio of the RMS at the n pulse over the RMS of the (n-2) pulse crossing a given threshold.
The gain on the response of the sensor, during a breakdown, has to be well adjusted to avoid saturation of the signal. Not doing so might lead to a wrong calculation of the RMS and inaccurate localization of the breakdown.

The results obtained from the T53VG3RA structure, where more than 75% of the breakdown are localized in the input couler, has led to rearrange the position of our sensors, Fig.14. It was believed that some breakdown were also happening in the arm of the waveguide. As a result a certain number of sensors were moved form the body of the structure to the arms and on the

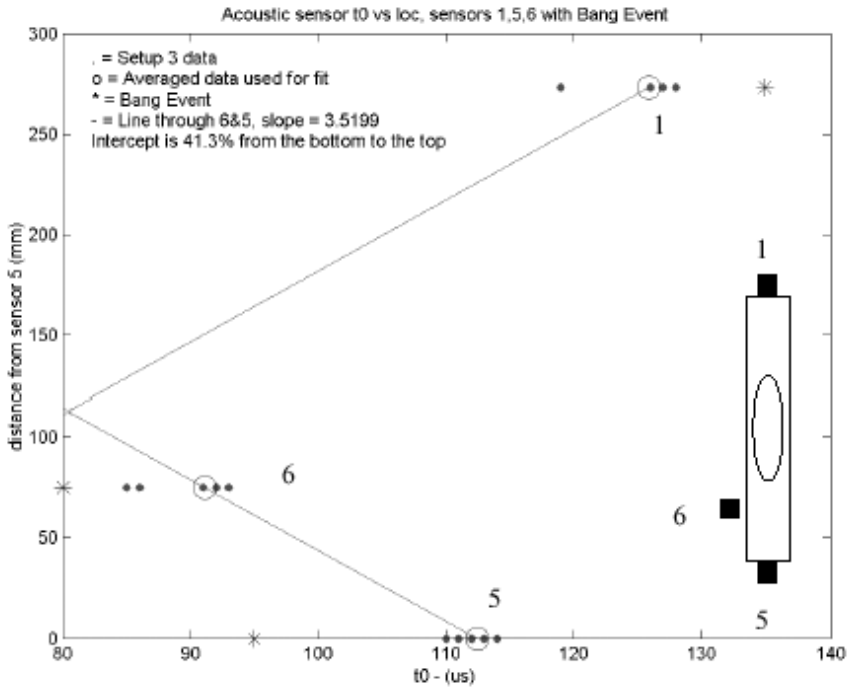

Figure 17. Sensor distance from sensor 5 vs t0 for the sensors mounted around the periphery of the rectangular waveguide at its connection point to the coupler cavity. The numerals indicate the sensor number with a top view of the waveguide, looking down from above, in the lower right hand corner of the figure showing approximate sensor locations. Sixteen events are indicated by the dot symbols and the single large bang event is indicated by *. The circles show the mean t0 of the 16 events. [18]

input coupler, Fig.18. The results of the acquisition is shown in Fig.19.

A clear asymmetry could be seen each time the input coupler was arcing. This asymmetry was similar to the video data recorded for one of the RF processed Standing Wave (SW) structure [19]. Since we start monitoring activity in structures, we found that most of the breakdown were localized at the beginning of the structure, Fig.14 (right) and Fig.20. Fig.20 localize single breakdown in the T105 (travelling wave structure of 105 cm long). Sensors are located every 6 cells starting at cell 2. The localization of every breakdown is done manually by analyzing every event and interpolating the timing and the height of the response of the sensors. Data shows clearly a serious problem in the input coupler, as well as the output coupler but in a less extend.

5.3 Implication of the Acoustic Results

Following the results obtained by the acoustic sensors on the localization of events during RF breakdown as shown for example in Fig.14, autopsies of the T53VG3R and T53VG3RA structure have been carried out [1]. Extreme

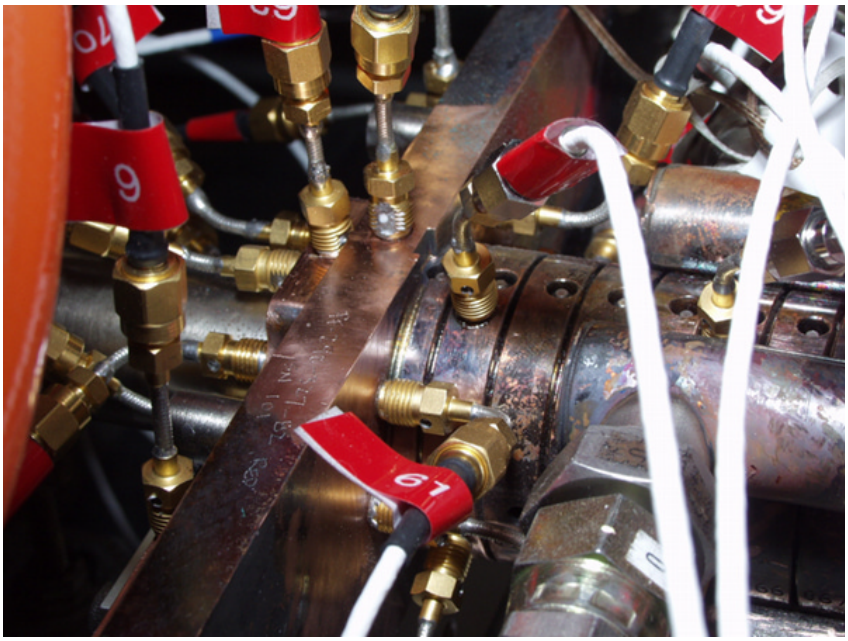

Figure 18. T53VG3RA structure input coupler closeup

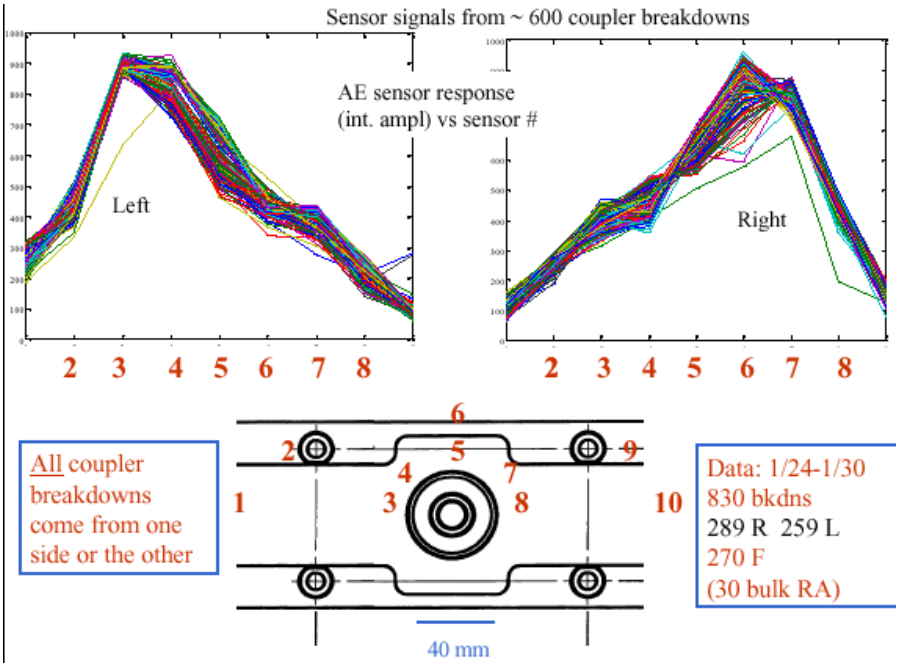

Figure 19. Localization of breakdown inside the input coupler of T53VG3RA

damages on the "horns" of the input coupler have been identified, cf Fig.22. The horns are the corner separating the waveguide from the cell, as shown in the schematic drawing in Fig.19. In another travelling wave structure (90 cm long 5% group velocity) one cell had more breakdowns than the neighboring cells, cf Fig.21. As the cross check between RF analysis and the acoustic measurement were not concordant. Visual inspection and an autopsy were performed. On the predicted cell, we discover more craters due to a more

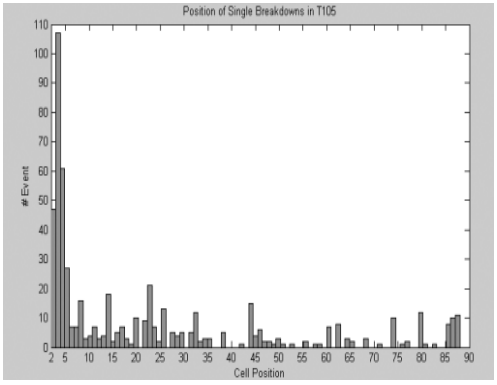

Figure 20. Manual localization of single breakdown inside T105VG5 at 240ns RF pulse length

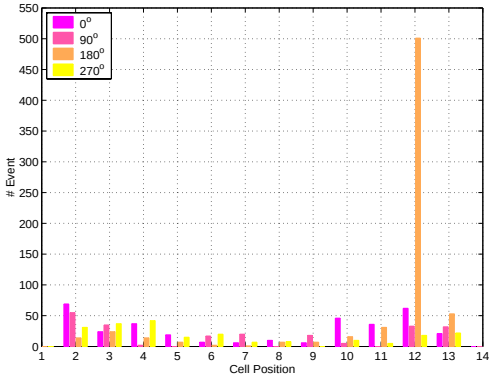

Figure 21. Position of RF Breakdown in H90VG5 after processing at 50ns, 100ns and 240ns pulse length. 4 sensors are located on each cell on the first 13^{th} cells.

intense activity as well as a piece of aluminium foil sitting on the bottom of the structure [20], labelled 180° in Fig.21. Sensors were located in a similar way as shown in Fig.1, 0° being the top of the structure.
The help of the autopsy as a validation of our localization method has led us to better understand the cause of the breakdown occurring inside the input couplers, and especially on the sharp edges of those horns [6]. A new design of the coupler as well as the cells has been implemented for the next structures. Results with the new design are extremely encouraging.

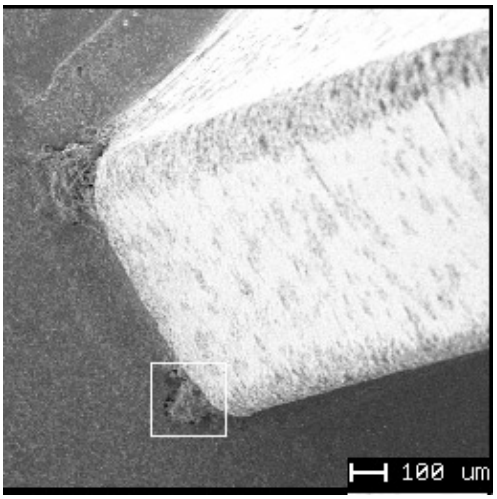

Figure 22. Autopsy of the Upper Right Horn of the T53VG3RA structure

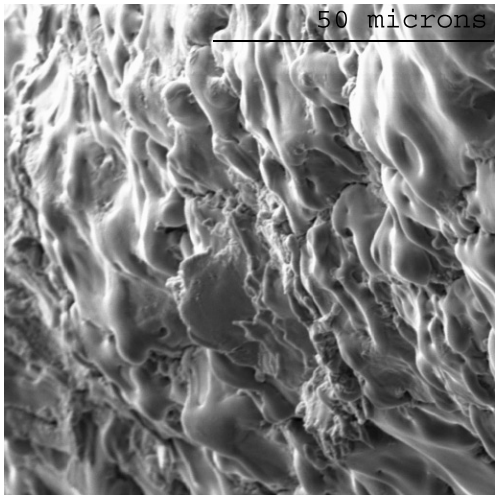

Figure 23. Typical damage on either edge of the horns, as represented in Fig.22

6 Conclusion

Localizing damage by the mean of ultrasonic wave is commonly used in aircraft and building industry. Applying massively this technique to localize RF

breakdown in accelerators device is rather new, and we have been able to successfully demonstrate this effectiveness. We have been able to also prove the complementarity of the acoustic detection to the conventional RF analysis.

One of the main results has been to identify that breakdown in the input coupler, of our test accelerating structure, were happening on the side of the coupler. With the help of surface analysis and some theoretical work [1] [6] [21] the structure has been redesigned. Localization of pieces of foreign materials inside the structures, has shed light on the handling procedures needed to keep the structures clean.

The next step in understanding breakdown by the mean of acoustic sensor, is to first have a good knowledge of the propagation of the acoustic waves in annealed copper, cf [**?**]. This understanding will help on accurate localization, as it is possible on superconductivity cavities [22]. Being able to do so is opening the door to know about the importance of particules contamination or smoothness of the surface in triggering breakdowns.
Understanding calibration is understanding the deposition of energy in an event, and being able to account for it. As a result we might have a clearer idea on the relation between damage (phase shift) in the structure and the deposited energy.

7 Acknowledgments

K. Luchini for help on data storage and data preprocessing. K. Ratcliffe contributions to the NLCTA structure program is also acknowledge. Finally, and despite the fact that ILC is going to be a cold machine, the lead author has still hope upon finalization of this paper for a real publication in NIM A ...

References

[1] F. Le Pimpec et al. Autopsy on an RF-Processed X-band Travelling Wave Structure. In *LINAC 2002, Korea*, 2002. SLAC-PUB-9526 .

[2] M. Gangeluk, et al. Acoustic Monitoring System of RF breakdowns Inside the Electrodynamics Structure at Kurchatov SR Source Accelerator. In *EPAC, P.1986*, 1994.

[3] NLC collaboration. 2001 Report on the Next Linear Collider. Technical report, SLAC-R-571, 2001.

[4] NLC ZDR Design Group. Technical report, SLAC Report-474, 1996.

[5] A.D Yeremian et al. Processing studies of X-band accelerator structures at the NLCTA. In *PAC, Vancouver Canada*, 1997.

[6] V. Dolgashev. Experiments on Gradient Limits for Normal Conducting Accelerators. In *LINAC 2002, Korea*, 2002.

[7] David R. Lide, editor. *Handbook of Chemistry and Physics*. 74^{th} edition. CRC PRESS, 1994.

[8] A. Zielinski. Ultrasonic Attenuation in Hydrogen Charged Copper Single Crystal. *Scripta Metallurgica et Materiala*, 24:527, 1990.

[9] J. and H. Krautkrämer. *Ultrasonic Testing of Materials*. Springer-Verlag, 1990.

[10] *Nondestructive Testing Handbook : Acoustic Emission*. 2nd edt, Volume 5. ASNT, 1987.

[11] J.P Wolfe. *Imaging Phonons Acoustic wave Propagation in Solids*. Cambridge, 1998.

[12] J. Frisch et al. Acoustic Measurement of RF Breakdown in High Gradient RF Structures. In *Linac 2000, USA*, 2000. SLAC-PUB-8580.

[13] J. Frisch et al. Studies of Breakdown in High Gradient X-band Accelerator Structures Using Acoustic Emission. In *Linac 2002, Korea*.

[14] Standard Method for Primary Calibration of Acoustic Emission Sensors. *ASTM international*, pages 536–547, 2002. E1106-86.

[15] P.R. Bevington, D.K. Robinson, editor. *Data Reduction and Error Analysis for the Physical Sciences*. McGraw-Hill, 1992.

[16] J. Tan. *Etude de L'émission Electronique par Effet de Champ en Haute Fréquences*. PhD thesis, Université Pierre et Marie Curie Paris 6, 1995.

[17] C. Adolphsen et al. Results of High Power Tests 30. In *ISG8*, 2002. http://www-project.slac.stanford.edu/lc/ilc/ ISG_Meetings/ISG8/wg4.htm.

[18] J. Nelson, M. Ross. Studies of TTF RF Photocathode Gun using Acoustic Sensors. Technical report, SLAC-PUB-9340, 2001.

[19] M. Ross et al. Measurement of RF Breakdown in X-band Structures. In *LC02 Workshop SLAC*, 2002. http://www-conf.slac.stanford.edu/lc02/wg2/WG2_Ross.pdf.

[20] S. Harvey et al. Surface Analysis of OFE-Copper X-Band Accelerating Structures and Possible Correlation to RF Breakdown Events. *Journal of Vacuum Science and Technology*, A22(4), 2004.

[21] D. Pritzkau. *RF Pulsed Heating*. PhD thesis, Stanford University, 2001. SLAC-report-577.

[22] J. Knobloch. *Advanced Thermometry Studies of Superconducting RF Cavities*. PhD thesis, Cornell University, 1997. http://w4.lns.cornell.edu/public/CESR/SRF/dissertations/knobloch/knobloch.html.

List of Figures